PRESSURE HISTORIES FROM THIN AND THICK SHOCK-INDUCED MELT VEINS IN METEORITES Zhidong Xie[1], Thomas G. Sharp[1], and Paul DeCarli[2], [1]Geological Sciences Department, Arizona State University, Tempe, AZ 85287, U.S.A. zhidong.xie@asu.edu, tom.sharp@asu.edu, [2]SRI International, 333 Ravenwood Ave., Menlo Park, CA 94025, paul.decarli@sri.com.

1. Introduction

Shock metamorphism, resulting from hypervelocity collisions, is a fundamental process in the early solar system [1-6]). The minerals that crystallized from the shock-induced melts provide a record of crystallization and quench histories that can be used to constrain shock pressure and pulse duration [3, 4, 7, 8]. Most previous investigations have focused on thick veins (> 100 μm in width) because they are observable using petrography and tend to contain high-pressure minerals [3, 4, 7, 8]. However, thin shock veins may contain complementary crystallization information. Shock veins cool predominantly by thermal conduction to the cooler host rock, resulting in quench times that are proportional to the vein thickness [5, 9-11]. Therefore, thin melt veins should quench faster than thicker veins and will record shorter crystallization histories.

If melt veins form during shock loading, the initial melt-vein crystallization, which occurs at the vein edge, should record the peak shock pressure. If veins crystallize during decompression, the crystallization assemblages should record a pressure drop from the initial crystallization at the vein edge to final crystallization of the vein center. The crystallization history of any shock vein will depend on vein thickness (quench rate) and on when it formed during the shock pulse.

The goal of this study is to test these predictions by determining the mineralogy of thin melt veins in shocked meteorites and comparing these results to those for thicker veins in the same samples.

2. Sample and Methods

We have investigated melt veins of various size in three L chondrites and one Martian meteorite. The samples include: Tenham (5, 8 and 30 μm veins), Roy (10 μm), Umbarger (35 μm) and Zagami (125 μm). Thicker veins in Tenham (600 μm wide), Roy (150 μm) and Umbarger (300 μm) have been previously investigated [12] and have mineral assemblages consistent with crystallization at approximately 25, 18 and 18 GPa for Tenham, Roy and Umbarger, respectively.

Transmission electron microscopy (TEM) imaging techniques were employed to characterize the microtexture of the veins and the microstructures of the vein minerals. Mineral phases were identified on the basis of selected area electron diffraction (SAED) and quantitative energy dispersive spectroscopy (EDS) microanalysis. Mineral assemblages in the melt vein matrix were used, in combination with phase relation data [13, 14] (Fig. 1), to constrain the crystallization pressure of the melt vein. The approach is not to assume chemical equilibrium and determine exact crystallization pressures and temperature from phase equilibrium data, but rather constrain the crystallization pressure from the overall pressure stabilities of the minerals that crystallized from the melt.

3. Results

3.1 Tenham

Tenham is a highly shocked (S6) L chondrite with many melt veins and pockets. A 580 μm wide melt vein of Tenham contains majorite and magnesiowüstite in the center of the melt vein, and ringwoodite, akimotoite, vitrified silicate-perovskite and majorite at the vein edge. Both mineral assemblages are consistent with a crystallization pressure ~25 GPa, but the vein-edge assemblage contains metastable phases [12, 15]. However, thinner veins show different mineral assemblages. A 5-μm wide melt vein contains predominantly silicate glass and metal-sulfide droplets, suggesting very rapid quench. An 8-μm wide vein consists of fine olivine crystals (200 nm in size) and metal-sulfide grains, suggesting crystallization at a pressure below 14 GPa (Fig. 1). A 35 μm wide vein contains majorite in the vein center and acicular olivine crystals in a local glassy matrix near the melt-vein edge. The majorite bearing assemblage is consistent with crystallization at ~22 GPa whereas the vein edge assemblage suggests very rapid quench and metastable crystallization of olivine.

3.2 Roy

Roy is an L chondrite with shock features ranging from S3 to S5. A thick melt vein (150 μm in width) in Roy contains majorite plus ringwoodite and clinopyroxene, consistent with a crystallization pressure ~ 18 GPa [12, 15]. However, a 10-μm wide melt vein of Roy contains low-Ca clinopyroxene and unidentified phases, suggesting crystallize pressure below 18 GPa (Fig. 1).

3.3 Umbarger

Umbarger is an L chondrite with shock effects reflecting shock stage S4 to S6. A 300-μm wide melt vein in Umbarger contains ringwoodite, akimotoite and clinopyroxene in the vein matrix, and Fe_2SiO_4-spinel and stishovite in SiO_2-FeO rich areas of the melt vein [12, 15]. These mineral assemblages are consistent with crystallization at ~18 GPa. A 30 μm wide melt vein contains ringwoodite, low-Ca clinopyroxene, and Ca-rich clinopyroxene, suggesting crystallization pressure at ~18 GPa (Fig. 1).

3.4 Zagami

Zagami is a Martian Shergotite with shock stage of S5-S6. A thin (~1 μm) and thick vein (~100 μm wide) were reported to contain various minerals that crystallized from the melt. They include omphacite, stishovite, hollandite-structured plagioclase, akimotoite, amorphous silicate perovskite and silicate titanite [5, 16], which were interpreted to crystallize during decompression from 25-5 GPa [5, 16]. Our Zagami sample has a 125 μm wide melt vein, which contains acicular stishovite crystals in a glassy matrix. In addition, maskelynite near the melt vein also contains α-PbO2-structured SiO_2 (Seifertite). Coexistence of Seifertite and stishovite, along with other minerals are indicative of crystallization at ~ 25 GPa, implying that extreme pressures are not needed to form Seifertite.

4. Discussion

Possible mechanisms for localized melting during shock compression include adiabatic shear, compression of locally porous regions, and shock collisions or jetting at fractures. The subsequent crystallization of silicate and metal-sulfide melts by thermal conduction with cooler host rock can occur at peak shock pressure, during pressure release, or after pressure release [9-12]. The basic assumption of our analysis is that the pressure-temperature history of a melt vein or melt pocket can be inferred from the assemblage of minerals that crystallize from the melt. High-pressure minerals are expected for cooling at high pressure; low-pressure minerals are expected for cooling at low pressure.

Our results show that in general, the minerals that crystallize in thin shock veins are not the same as those in thicker veins in the same samples and the thin-vein assemblages generally imply lower crystallization pressures. There are three likely explanations for this. The first is that the thinner veins could be injection veins that form in fractures that open during pressure release. If this were the case, such veins would have to tap the liquid contents of larger veins or melt pockets that are still liquid during or after pressure release. This seems unlikely since we do not find similar low-pressure assemblages in the centers of large veins. A second alternative is that these samples have multiple generations of shock veins and that the thin veins may represent a lower pressure shock event. This may be the case for Tenham, where some textural evidences suggest two phases of vein formation. Finally, the thinnest melt veins, which quench fastest, are likely to be supercooled and crystallize metastable phases or quench glass. The presence of metastable akimotoite at the margins of melt veins in Umbarger and Tenham indicates that rapid quench does produce metastable phases. The results of this study suggest that the best melt veins for interpreting crystallization pressures are the thicker veins that are quenched more slowly and generally have assemblages that are consistent with published phase diagrams.

References: [1] Chao, E.C.T. (1967) *Science 156*, 192-202. [2] Stöffler, D. et al. (1991) *GCA 55*. 3845-3867. [3] Chen, M. et al. (1996) *Science 271*. 1570-1573. [4] Sharp, T.G. et al. (1997) *Science 277*, 352-355. [5] Langenhorst, F. and Poirier, J.P. (2000) *EPSL 184*, 37-55. [6] Leroux, H. (2001) *EJM 13*, 253-272. [7] Tomioka, N. and Fujino, K.(1997) *Science 277*, 1084-1086. [8] Xie, Z. et al. (2002) *American Mineralogist 87*, 1257-1260. [9] Sharp T.G. et al. (2003) *LPS XXXIV*. 1278.pdf. [10] DeCarli, P. et al. (2001) *APS conference of Shock Compression of Condensed Matter 2001*, 1381-1384. [11] DeCarli, P. et al. (2003) *APS conference of Shock Compression of Condensed Matter 2003*, 1427-1430. [12] Xie, Z. (2003) *Dissertation*. [13] Agee C. B. et al. (1995) *JGR,100,* 17,725-17,740. [14] Zhang, J. and Herzberg, C. (1994) *JGR 99*, 17729-17742. [15] Xie Z. et al. (2003) *LPS* XXXIV, 1280.pdf. [16] Langenhorst, F. and Poirier, J.P. (2000) *EPSL 176*, 259-265.

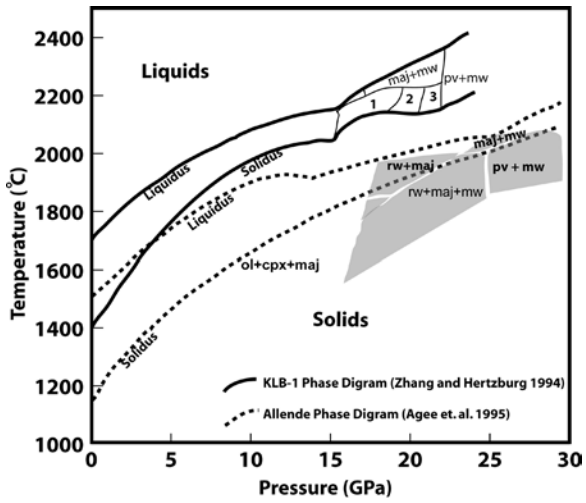

Fig. 1 Combined and simplified versions of the Allende phase diagram (Agee et al. 1995) and KLB-1 phase diagram (Zhang and Hertzburg 1994). ol = olivine, cpx = clinopyroxene, rw = ringwoodite, maj = majorite, mw = magnesiowüstite, pv =perovskite, 1 = liquid + majorite + wadsleyite, 2 = liquid + majorite + wadsleyite + magnesiowüstite, 3 = liquid + majorite + magnesiowüstite + ringwoodite + Ca-perovskite.